SOME NEW ASPECTS OF BIMODAL FISSION IN ^{258}Fm ISOTOPE

A. STASZCZAK and Z. ŁOJEWSKI

Department of Theoretical Physics, M. Curie–Skłodowska University
pl. M. Curie–Skłodowskiej 1, 20–031 Lublin, Poland

Abstract

Using the multidimensional dynamic–programming method (MDPM) in the four–dimensional deformation space $\{\beta_\lambda\}$ with λ=2, 4, 35 and 6 we were able to study evolution of the action integral of the fissioning nucleus ^{258}Fm. We found the second minimum on the cross–section of the action integral for $\beta_2 \approx 1$, what we interpret as the dynamical evidence of the bimodal fission in this heavy Fm isotope.

1   Introduction

Experimentally known values of the spontaneous fission half–lives T_{sf} of nine even–even Fm isotopes (N = 142, 144, ..., 158) form approximately two sides of an acute–angled triangle with a vertex in N = 152. The rapid changes in T_{sf} on both sides of ^{252}Fm are particularly dramatic for the heavier Fm isotopes, where T_{sf} descends by about ten orders of magnitude when one passes from ^{254}Fm to ^{258}Fm.

Nuclei in the vicinity of ^{258}Fm reveal another two peculiarities in spontaneous fission properties. The fission process becomes symmetric with the narrow mass distributions (see e.g. review [1]) and the total–kinetic–energy (TKE) distributions are not Gaussian, but instead are best described as a sum of two Gaussians. For ^{258}Fm the TKE distribution has peaks at about 200 and 235 MeV. It was postulated [2] that for ^{258}Fm the observed high–kinetic–energy peak corresponds to fission through a scission configuration of two touching spherical fragments, with the maximum of Coulomb repulsion. The low–kinetic–energy peak was thought to correspond to fission through a conventional scission configuration of two elongated fragments.

The investigations focused on a multi–valley structure of potential–energy surfaces for nuclei near Fm have been undertaken by a lot of authors. A particularly detailed studies were performed by a Los Alamos group [3, 4, 5] and

a Warsaw group [6, 7]. Comparison of used models and results obtained by the both groups one may find in [5] and in a review [8].

The descriptions of the bimodal fission in ^{258}Fm proposed by the Los Alamos and Warsaw groups are very similar. Roughly speaking in both cases authors present two fission path on the potential–energy surfaces. One trajectory goes into the valley which corresponds to more compact shapes (CS) of the nucleus and the other to the valley which corresponds to more elongated shapes (ES). However, the both presented descriptions of the bimodal fission have one common deficiency — they are totally static, focused only on the multi–valley structure of potential–energy surfaces.

The main goal of this paper is to present a dynamic analysis of the bimodal fission in ^{258}Fm. Thus, we focused our attention on an action–integral of the fissioning nucleus in a multi–dimensional deformation space.

The used model is described in sect. 2, the results and discussion are given in sect. 3.

2   Model

To calculate the action–integral along a path $L(s)$ in the multi–dimensional deformation space $\{X_\lambda\}$ we used the one–dimensional WKB semiclassical approximation

$$S(L) = \int_{s_1}^{s_2} \left\{ \frac{2}{\hbar^2} B_{\text{eff}}(s)[V(s) - E] \right\}^{1//2} ds \,, \tag{1}$$

where an effective inertia associated with the fission motion along the path $L(s)$ is

$$B_{\text{eff}}(s) = \sum_{\lambda,\mu} B_{X_\lambda X_\mu} \frac{dX_\lambda}{ds} \frac{dX_\mu}{ds} \,. \tag{2}$$

In above equations ds defines the element of the path length in the $\{X_\lambda\}$ space. The integration limits s_1 and s_2 correspond to the entrance and exit points of the barrier $V(s)$, determined by a condition $V(s) = E$, where E is the penetration energy of the fissioning nucleus.

The potential energy V is calculated by the macroscopic–microscopic model exactly the same like that used by the Warsaw group [7]. For the macroscopic part we used the Yukawa–plus–exponential finite–range model [9] and for microscopic part the Strutinsky shell correction, based on the Woods–Saxon single–particle potential with "universal" variant of the parameters [10]. The single–particle potential is extended to involve residual pairing interaction, which is treated in the BCS approximation. The inertia tensor $B_{X_\lambda X_\lambda}$, which

describes the inertia of the nucleus with respect to change of its shape, is calculated in the cranking approximation (cf. e.g. [11]). The penetration energy $E = V(X_\lambda^0) + 0.5$ MeV is defined as a sum of a ground–state energy $V(X_\lambda^0)$ at the equilibrium deformation X_λ^0 and a zero–point energy in the fission direction, equal 0.5 MeV.

Dynamic calculations of the spontaneous fission half–lives T_{sf} are understood as a quest for a least–action trajectory $L_{\min}$ which fulfills a principle of least–action $\delta[S(L)] = 0$. To minimize the action integral (1) we used the multidimensional dynamic–programming method (MDPM). Originally this method was used only for two–dimensional deformation space [11]. We extended the model up to four degrees of freedom.

The schematic Fig. 1 demonstrates how our model, the MDPM, works. Since the macroscopic–microscopic method is not analytical, it is necessary to calculate the potential energy and all components of the inertia tensor on a grid in the multidimensional space spreaded by a set of deformation parameters $\{X_\lambda\}$. We select one coordinate X_0 from this set. This coordinate (e.g. elongation parameter) is related in a linear way to the fission process. In Fig. 1 for each point on a X_0 axis the rest of the coordinates $\{X_{\lambda-1}\}$ are represented for simplicity by a "wall–plane" of only two coordinates X_1 and X_2.

To find the least–action trajectory $L_{\min}$ between the turning point s_1 and s_2 we proceed as follows. First, from the entrance point to the barrier s_1 we calculate the action–integrals to all grid points in the nearest "wall" at $X_0 = 1$. In the next step we come to the "wall" at $X_0 = 2$ and from each grid point in this "wall" calculate the action–integrals to all grid points in the "wall" at $X_0 = 1$ (see Fig. 1). The trajectories started from each grid point at $X_0 = 2$ passing through all grid points in "wall" at $X_0 = 1$ and terminated in the point s_1 form a bunch of paths. From each such a bunch we choose the path with minimal action–integral and keep them in the memory. At the end of this step we have the least–action integrals along trajectories which connect the starting point s_1 with all grid points in the "wall" at $X_0 = 2$. After that we repeat this procedure for all grid points at $X_0 = 3$ and again we obtain all least–action–integrals along trajectories starting from point s_1 with ends at each grid point in the "wall" $X_0 = 3$. We repeat it until we exceed the n–th "wall"; a last one before the exit point from the barrier s_2. After that we proceed to the last step of our method. We calculate action–integrals between all grid points in the last "wall" at $X_0 = n$ and the exit point s_2; the minimal one among them corresponds to the searched trajectory of the least–action–integral $L_{\min}$.

Our dynamical calculations are performed in the four–dimensional defor-

mation space spread by β–shape parameters appearing in an expansion of a nuclear radius in spherical harmonics. So, we have $\{X_\lambda\} \equiv \{\beta_\lambda\}$, with $\lambda = 2,4,35$ and 6. Our deformation space is very similar to used in ref. [7]. However, in opposite to ref. [7], we collect the reflection–asymmetry parameters β_3 and β_5 in one parameter $\beta_{35} \equiv (\beta_3, \beta_5=0.8\beta_3)$, according to the average trajectory in a (β_3, β_5) plane for nuclei in Fm region.

The potential energy V and ten components of the symmetric inertia tensor $B_{\beta_\lambda \beta_\lambda}$ are calculated microscopically for

$$\beta_2 = 0.15(0.05)1.30 \, ,^1$$
$$\beta_4 = -0.08(0.04)0.36 \, ,$$
$$\beta_{35} = 0.00(0.05)0.25 \, ,$$
$$\beta_6 = -0.12(0.04)0.12$$

(3)

i.e. in the $24 \times 12 \times 6 \times 7 = 12096$ grid points. In our calculation a quadrupole deformation β_2 plays a role of the coordinate X_0 from Fig. 1.

3   Results and discussion

Fig. 2 displays the cross–sections of the action–integral (in units of $\hbar$) of the nucleus ^{258}Fm, obtained according to our MDPM model for the different values of parameter β_2. To show a three–dimensional structure of these cross–sections we reduced the results to the two–dimensional (β_4, β_{35}) contour plots. This we accomplish by plotting at each point a minimal value of action–integral with respect to a third coordinate β_6. Thus, in Fig. 2 one can see an evolution of the action–integral in the fission process of ^{258}Fm.

The two–dimensional contour diagrams show fairly smooth surfaces with one minimum. On all contour diagrams a position of the minimum, in a lower–left corner, is almost the same. If we join the minima from all contour maps, we obtain a dynamical fission trajectory in our four–dimensional deformation space. The dynamical fission trajectory has a tendency to be close to a straight line. It means a reduction of the effective inertia B_{eff} according to eq. (2) and leads to the smaller action–integral. This dynamical fission trajectory goes to the compact shapes (CS) (cf. e.g. Fig. 6 in ref. [7]).

In the last contour map in Fig. 2 with the cross–section of the action–integral for $\beta_2 = 1.05$ one can see in an upper–right corner a second local minimum corresponding to more elongated shapes (ES). This second local

---

[1]Here we use the notation $x = x_i(\Delta x)x_f$ which means that x goes from x_i through x_f with step Δx.

minimum is more distinctly seen in Fig. 3 where we plot a contour diagram of the action–integral obtained in the last step of the MDPM, when we calculate the action–integral from all grid points on last "wall" to the exit point from the barrier s_2 (see Fig. 1). In other words, in Fig. 3 we show a "view" of the last "wall" at $\beta_2 = 1.05$ "seen" from the exit point s_2 with coordinates: ($\beta_2 = 1.10$, $\beta_4 = 0.05$, $\beta_{35} = 0.01$, $\beta_6 = -0.06$). The appearance of two minima on the cross–section of the action integral, one global corresponding to more compact shapes (CS) and another local corresponding to more elongated shapes (ES), indicates that in the vicinity of $\beta_2 = 1.05$, before the exit from the barrier, one can observe the begining of the two fission modes in ^{258}Fm .

Fig. 4 shows the potential energy V calculated for ^{258}Fm as a function of the deformation parameters β_2 and β_4. At each point (β_2, β_4) we select the value of $V(\beta_2, \beta_4, \beta_{35}, \beta_6)$ minimal with respect to β_{35} and β_6, where β_{35} and β_6 are taken only from the grid points, according to (3). On the right part of the figure one can see two valleys. Entrances to the valleys of compact and elongated scission shapes are denoted by CS and by ES, respectively.

Fig. 4 also includes paths to fission. A nearly stright, solid line, which starts in the first minimum (at $\beta_2 \approx 0.25$, $\beta_4 \approx 0.0$) and goes to the CS valley, represents the dynamical fission trajectory leading to compact shapes. From this trajectory, close to the exit point from the barrier (at $\beta_2 \approx 0.95$, $\beta_4 \approx 0.05$), the fission trajectory leading to the ES valley branches off (a dotted–dashed line).

Only for comparison we display in Fig. 4 a static fission trajectory (i.e. the path of minimal potential energy for each β_2 value), shown as a dashed line. This trajectory starts in the first minimum, passes through the first saddle point (at $\beta_2 \approx 0.4$, $\beta_4 \approx 0.1$), then through the second minimum (at $\beta_2 \approx 0.65$, $\beta_4 \approx 0.05$), through the second saddle point (at $\beta_2 \approx 0.85$, $\beta_4 \approx 0.05$), and leads to the valley of elongated scission shapes.

All fission barriers along the static and both dynamical trajectories in Fig. 4 have two humps, in distinction to ref.[7] where the static barrier has only one hump. This difference, despite the similar macroscopic–microscopic models used, seems to come from minimization procedure of the total energy of the nucleus in the multidimensional deformation space applayed by the Warsaw grup in [7].

Our results of bimodal fission in ^{258}Fm are in agreement with those obtained by the Los Alamos group [3, 4, 5, 8], where the splitting of the trajectories appears also a little befor the exit point from the barrier. This is in opposite to the Warsaw group [6, 7] description where the fission trajectory splits behind the exit point from the barrier.

5

References

[1] P. C. Hoffman, *Accounts Chem. Res.* **17**, 235 (1984).

[2] E. K. Hulet, J. F. Wild, R. J. Dougan *et al.*, *Phys. Rev. Lett.* **56**, 313 (1986).

[3] P. Möller, J. R. Nix and W. J. Swiatecki, Proc. Int. School–Seminar on Heavy Ion Physics, Dubna 1986, JINR Report JINR–D7–87–68, 167 (1987).

[4] P. Möller, J. R. Nix and W. J. Swiatecki, *Nucl. Phys.* **A469**, 1 (1987).

[5] P. Möller, J. R. Nix and W. J. Swiatecki, *Nucl. Phys.* **A492**, 349 (1989).

[6] S. Ćwiok, P. Rozmej and A. Sobiczewski, Proc. 5th Int. Conf. on Nuclei far from Stability, Rosseau Lake 1987, ed. I. S. Towner (AIP Conf. Proc. 164, New York 1988), p. 821.

[7] S. Ćwiok, P. Rozmej, A. Sobiczewski and Z. Patyk, *Nucl. Phys.* **A491**, 281 (1989).

[8] P. Möller and J. R. Nix, *J. Phys. G: Nucl. Part. Phys.* **20**, 1681 (1994).

[9] H. J. Krappe, J. R. Nix and A. J. Sierk, *Phys. Rev.* **C20**, 992 (1979).

[10] S. Ćwiok, J. Dudek, W. Nazarewicz, J. Skalski and T. Werner, *Comp. Phys. Commun.* **46**, 379 (1987).

[11] A. Baran, K. Pomorski, A. Łukasiak and A. Sobiczewski, *Nucl. Phys.* **A361**, 83 (1981).
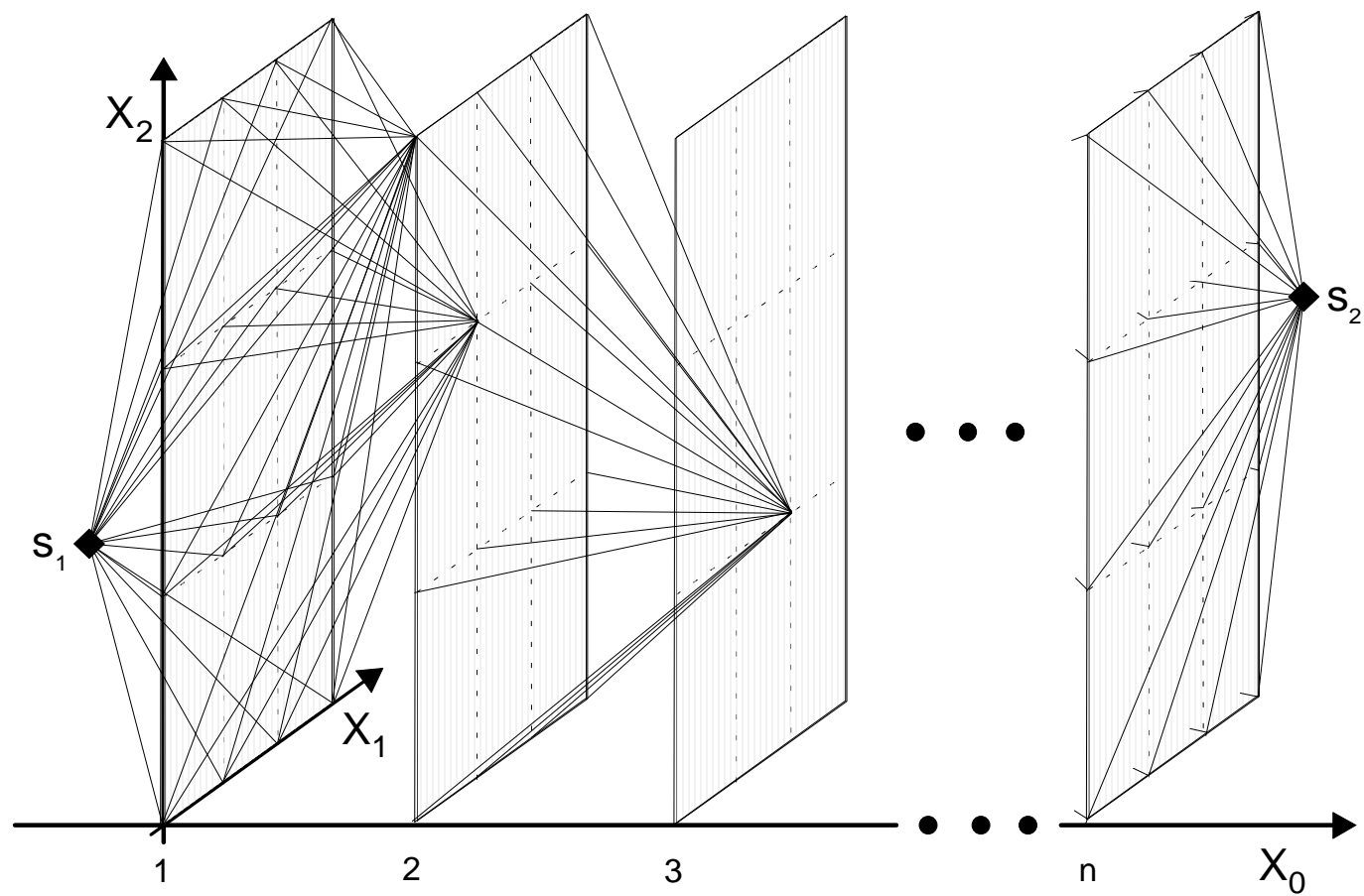
Figures Captions

Figure 1: Schematic presentation of the MDPM method. In the multidimensional deformation space $\{X_\lambda\}$ we select the coordinate $\{X_0\}$ which is related in a linear way to the fission process. The points s_1 and s_2 correspond to entrance to the barrier and exit from the barrier, respectively. See text for details.

Figure 2: Evolution of the action–integral in the fission process of ^{258}Fm. Each contour map represents cross–sections of the action–integral, in $\hbar$ units, obtained for the different values of parameter β_2.

Figure 3: View of the last contour map from Fig. 2, with cross–section of the action–integral at $\beta_2 = 1.05$, "seen" from the exit from the barrier point s_2. The letters CS indicate global minimum corresponding to more compact shapes, ES indicate second local minimum corresponging to more elongated shapes.

Figure 4: Contour map of the potential energy of ^{258}Fm, showing paths to fission. Solid line represents the dynamical fission trajectory leading to compact shapes (CS), the dotted–dashed line denotes branches off second dynamical trajectory leading to elongated shapes (ES). The dashed line represents the static fission trajectory.

$$\{X_\lambda\} = X_0 \oplus \{X_{\lambda-1}\}$$

^{258}Fm
Potential energy [MeV]